Journal of Multidisciplinary Engineering Science and Technology (JMEST)
ISSN: 3159-0040
Vol. 2 Issue 6, June - 2015

Bond Strength of Ribbed GFRP Bars Embedded in High Performance Fiber Reinforced Concrete

K.M.A. Hossain and K. Sennah
Department of Civil Engineering, Ryerson University,
Toronto, Canada
ahossain@ryerson.ca

A.A.A. Hamoda
Structural Eng. Dept., Kafr El-Sheikh University,
Kafr El-Sheikh, Egypt
M.E.S. Shoukry and Z.I. Mahmoud
Structural Eng. Dept., Alexandria University,
Alexandria, Egypt

***Abstract*—The use of prefabricated bridge construction is an emerging and growing technology in USA and Canada. In this accelerated construction, simple units of pre-cast slabs are connected to each other by closure strips made of glass fiber reinforced polymer (GFRP) bar and high performance concrete (HPC). The pullout bond strength of GFRP bar embedded in HPC material is very important for the design of such closure strips. Emerging fiber reinforced Engineered Cementitious Composite (ECC) with its intrinsically tight crack width associated with high tensile ductility is an ideal material for closure strip construction. This paper presents the bond strength of GFRP bars embedded in ECC and traditional Fiber Reinforced Concrete (FRC) based on pullout tests conducted on 32 specimens. The variables included are: bar configuration (straight and headed end bar), bar location (central and eccentric), concrete type (ECC and FRC) and embedment length (4, 6 and 8 times bar diameter). The influences of each of these variables on bond strength are described. All specimens exhibited pullout mode of failure with ECC specimens showing significantly higher ductility compared to their FRC counterparts. The bond strength of headed end GFRP bar was significantly higher compared to that of straight bar and the pullout load increased with the increase of embedment length. Bond strengths derived from existing Code based design equations are compared with those obtained from experiments.**

***Keywords*—bond strength; pullout test; GFRP bar; codes; engineered cementitious composite**

I. INTRODUCTION

Full-depth, full width, precast concrete deck slabs placed transversally over steel or concrete girders have recently been used in Canada and America for accelerated bridge construction. It offers many economic, safety and functional benefits. Prefabricated bridge elements and systems range from simple girders, bent caps and deck panels to substructure and superstructure units. They are manufactured on-site or off-site, under controlled conditions and brought to the job location ready to install. Prefabricated components have been shown to be efficient, durable and require much reduced site-construction time. Growing traffic on the highways and increasing user delays due to construction zone restrictions are challenging bridge designers and builders to find ways to build bridges faster and minimize traffic delay, community disruption and exposure to construction hazards. With the use of prefabricated bridge elements and systems in the construction of new bridges and the replacement of old ones, the more frequent traffic lane closure will be considerably reduced, reflecting in reduction in transportation related greenhouse gas emission (GHG).

In this prefabrication, simple units of pre-cast slabs are connected to the side of each other, over girders, using fillers of high performance concrete (HPC) materials given the final shape of full-depth, full width, precast concrete deck slabs as shown in Fig.1.

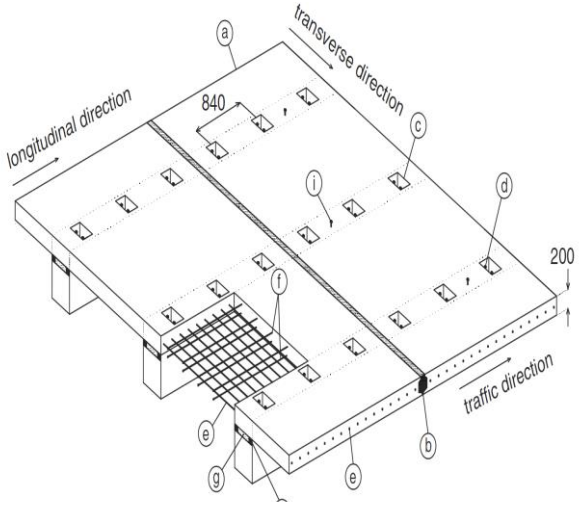

a - concrete precast prestressed panels; b – closure strip; c - composite pockets; d- shear connectors; e - FRP bars in the transverse direction; f- FRP bars in the longitudinal direction; g- haunch; h - compressible foam; i- leveling bolts; *dimensions in mm*

Fig. 1. *Precast concrete bridge deck slab with full-depth precast prestressed panels [1]*

The glass fiber reinforced polymer (GFRP) bar reinforced HPC closure strip between the jointed slabs is an emerging technology and use of this technology can enhance strength and durability leading to sustainable construction. The design of the joint between full-depth precast deck slabs supported over girder in accelerated bridge construction requires the pullout bond strength of GFRP bars embedded in the HPC closure strip.

During the last decades, tremendous progress has been made on the HPCs. Such HPC technology involves the family of highly durable fibre reinforced engineered cementitious composites (ECCs) besides traditional fiber reinforced concrete (FRC). ECC is characterized by excellent strain capacity under uniaxial tension, multiple cracking and moderate fiber volume fraction (typically 2%) [2,3]. Compared with ordinary concrete material, ECC can strain harden after first cracking, similar to a ductile metal and demonstrate a strain capacity of 300–500 times greater than normal concrete [4]. Like most FRCs, ECC exhibits self-controlled crack width under increasing load. Even at large deformation, crack widths of EC remain less than 60 μm [2, 5-7].

Concrete failure is associated with the brittle fracture of the concrete due to the high stress concentration induced by the headed reinforcing bars normally used to reduce the development length and hence to reduce the width of the closure strips in pre-fabricated bridge. Improved concrete toughness and tensile ductility are expected to enhance anchor capacity. ECC with its intrinsically tight crack width associated with high tensile ductility is the ideal material for such construction.

Increasing the tensile strength of concrete is one of the main reasons of incorporating fibers. Post cracking resistance of the concrete is also improved by reinforcing the concrete with fiber which could be very important in structures where crack control is an issue. When failure occurs, fibers are pulled out of the concrete leading to an increase in the energy needed to open the cracks [8,9]. Steel bars embedded in FRC members with only 2% fiber showed an increase of 55% in bond strength. On the other hand, it is illustrated that the application of steel fibers will lead to bond strength reduction of up to 30% in normal strength concrete and 16% in high strength concrete [10]. The reason was attributed to the local stress disturbance caused by fibers preventing proper compaction around the rebar and therefore, reducing bond strength. In high strength concrete, disturbance was less distinct in comparison with normal concrete [11]. Moreover, the influence of synthetic and steel fibers on high strength concrete and FRP bars was experimentally studied [12]. The bond strength between the concrete and FRP bars can be increased from 5 to 70% by increasing the fiber content in the concrete.

The design of the joint between full-depth precast deck slabs supported over girder in accelerated bridge construction requires the pullout strength of glass fiber reinforced polymer (GFRP) bars embedded in the closure strip. Bond strength FRP bars have been investigated in many research studies [12-15]. However, little or no research has been conducted on the bond strength of GFRP/FRP bars embedded in ECC.

This paper presents the results of an investigation on the bond characteristics between GFRP bars and the filler of high performance concrete materials used in the closure strip. Tests were conducted by using pullout specimens having variable parameters such as: embedded length, type of filler material (ECC and FRC), bar location and end case (straight or headed end bar). The influences of each of these parameters on bond strength are described. Bond strengths derived from existing Code based design equations are compared with those obtained from experiments. This research has practical significance as it contributes to an important aspect of GFRP reinforced ECC technology where knowledge is not available and provides data for the Code writers and professionals. The findings and conclusions of this research will surely benefit engineers, builders and local authorities involved in designing and constructing pre-fabricated bridges with GFRP reinforced ECC closure strips.

II. Experimental Program

A. Material Properties

Two concrete mixes namely ECC and FRC were used to cast pullout specimens. Flowable ECC was made of Poly vinyl alcohol (PVA) fiber, silica sand, Portland cement, fly ash and admixtures with a water to binder ratio of 0.27. Conventional non-flowable FRC was made of Portland cement, steel fiber, silica fume, local sand, air-entraining admixture and 10 mm maximum size stone. The compressive strength of the concrete was determined from the average of four 100 × 200 mm cylinders that were cast and cured under the same laboratory conditions as the pullout specimens and tested at the time of pullout tests. The average value of compressive strength of ECC and FRC was about 55 MPa and 75 MPa, respectively. ECC specimens were cast without consolidation while external compaction was applied for FRC specimens.

Fig.2. *GFRP bars (straight and headed end)*

16 mm diameter ribbed GFRP bars with specified tensile strength of 1105 MPa, modulus of elasticity of 64.7 ± 2.5 GPa and strain at rupture of 1.71% were used [16]. The same ribbed GFRP bar was used with (straight) and without headed-end as shown in Fig. 2.

B. Pullout Speceimens and Test Scheme

Thirty two pullout specimens having dimensions of 150 x150 x1 50 mm, 150 x 150 x 200 mm and 150 x 150 x 200 mm were constructed for straight and headed bars. Headed end bars were only used 4D (4 x bar diameter) specimens. The dimensions and placement of GFRP bars in the forms for the tested specimens are shown in Fig. 3 and Table. 1. The test program consisted of two groups (based on ECC and FRC) of pullout specimens as indicated in Table 1 with specimen designations and explanations.

Table 1. Details of Pullout Specimens: Variable and Designations

Specimen Designation	Size of Pullout Specimen (mm x mm x mm)	
F or E4H_0C	200 x 200 x 200	F: FRC E: ECC H: headed bar S: straight bar X: eccentric C: concentric D: bar diameter L_d: embedded length
F or E4H_{ld}C	200 x 200 x 200	
F or E4SC	150 x 150 x 150	
F or E4SX	150 x 150 x 150	
F or E6SC	150 x 150 x 150	
F or E6SX	150 x 150 x 150	
F or E8SC	150 x 150 x 200	
F or E8SX	150 x 150 x 200	

Group I consisted of eight specimens and these were duplicated to give sixteen ECC blocks designated as E4H_0C, E4H_{ld}C, E4SX, E4SC, E6SX, E6SC, E8SX and E8SC. Specimen E4H_0C had headed end bar without embedded length. Specimen E4H_{ld}C had headed end bar with embedded length equaled to 4D. Specimen E4SX had eccentric straight bar with embedded length equaled to 4D. Specimen E4SC had center straight bar with embedded length equaled to 4D. Specimen E6SX had eccentric straight bar with embedded length equaled to 6D. Specimen E6SC had center straight bar with embedded length equaled to 6D. Specimen E8SX had eccentric straight bar with embedded length of 8D.

Group II consisted of eight specimens and these were duplicated to give sixteen FRC tested specimens designated as F4H_0C, F4H_{ld}C, F4SX, F4SC, F6SX, F6SC, F8SX and F8SC. Specimen F4H_0C had headed end without embedded length. Specimen F4H_{ld}C had headed end with embedded length equaled to 4D. Specimen F4SX had eccentric straight bar with embedded length equaled to 4D. Specimen F4SC had center straight bar with embedded length equaled to 4D. Specimen F6SX had eccentric straight bar with embedded length equaled to 6D. Specimen F6SC had center straight bar with embedded length equaled to 6D. Specimen F8SX had eccentric straight bar with embedded length equaled to 8D.

Table 1 gives details of the tested specimens. In the name designation of specimens, F and E represent FRC and ECC, respectively, S and H represents straight and headed bar, respectively, X and C represent eccentric and concentric bar locations, respectively.

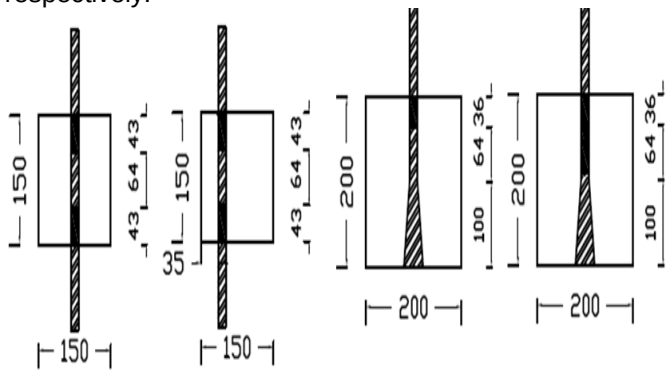

(a) 4D specimens

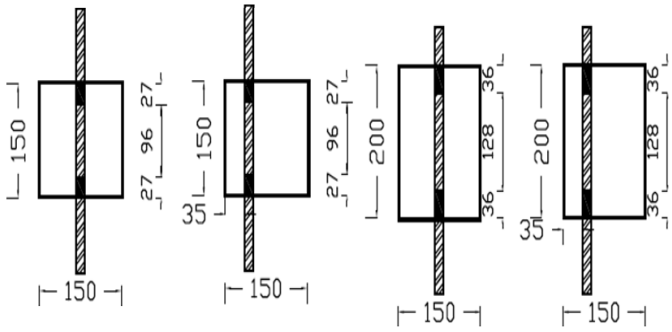

(b) 6D specimens (c) 8D specimens

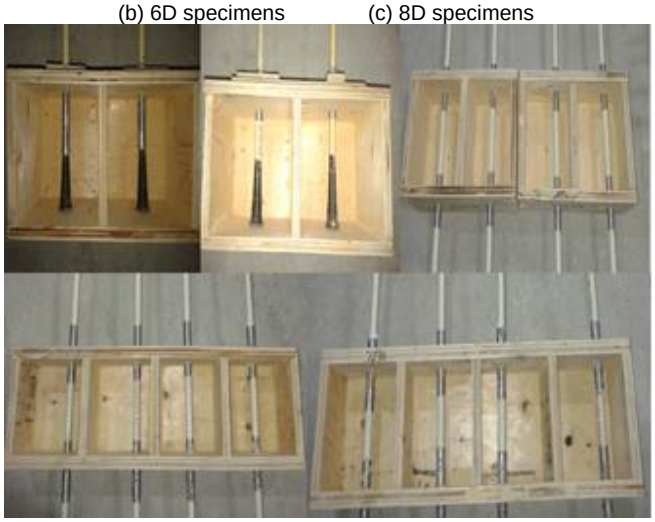

(d) Placement of GFRP bars in the forms

Fig. 3. *Dimensions and placement of GFRP bars in the forms (Dimensions in mm)*

Fig. 4. *Pullout test set-up*

C. Test Set-up and Testing

The pullout specimens were tested according to RILEM specification [17]. In the test setup, two LVDTs were strategically placed to measure the load end-slip and free end-slip of the bar. A hydraulic jack was used to exert the necessary pullout load with the hollow load cell located between this jack and the block to record the applied load. Slip was measured at two different locations, namely: (i) the loaded end-slip (LES) to measure the relative slip and bar elongation from the embedded side, and (ii) the free end-slip (FES) to measure the pure pullout of the bar. Test set-up is shown in Fig. 4. The load was applied based on the recommendation provided in CSA S806 [18] at a rate of 60 kN/min. The loading continued until the specimen failed.

Table 2. Test results for ECC specimens

Spec. Name	l_d	Peak Load (kN)	Mean	Bond Stress (MPa)	Mean	Slip (mm) LES	FES
$E4H_0C$	head	101	110	20.3	21.9	18.6	2.51
		119		23.6		23.1	0.75
$E4H_{ld}C$	head +4D	142	148	17.2	17.9	16.6	0.31
		154		18.7		22.7	0.67
E4SC	4D	22.5	20.8	7.0	6.5	4.7	0.02
		19.0		6.0		3.7	0.11
E4SX		19.0	23.6	6.0	7.3	5.3	0.46
		28.3		8.8		3.2	0.02
E6SC	6D	30.0	27.5	6.2	5.7	4.4	0.37
		25.0		5.2		5.0	0.73
E6SX		35.5	37.0	7.4	7.7	3.7	0.35
		38.5		8.0		5.8	0.27
E8SC	8D	56.0	56.0	8.7	8.7	1.8	0.17
		~~35.5~~		~~5.5~~		~~4.5~~	~~0.34~~
E8SX		59.8	60.4	9.3	9.4	6.8	0.12
Mean of two tests; LES: loaded end slip; FES: free end slip							

Table 3. Test results for FRC specimens

Spec. Name	l_d	Peak Load (kN)	Mean	Bond Stress (MPa)	Mean	Slip (mm) LES	FES
$F4H_0C$	head	117	118	23.2	23.4	15.1	0.29
		119		23.5		20.5	0.38
$F4H_{ld}C$	head+ 4D	167	170	20.3	20.7	17.5	0.17
		174		21.1		14.0	0.54
F4SC	4D	54.5	52.8	17.0	16.4	10.1	0.63
		51.0		15.9		7.0	0.28
F4SX		62.0	58.6	19.3	18.2	9.7	0.29
		55.3		17.2		11.4	0.46
F6SC	6D	62.3	61.3	13.0	12.7	9.5	0.25
		60.3		12.5		8.6	0.72
F6SX		68.5	63.0	14.3	13.1	9.0	0.49
		57.3		11.9		6.1	0.47
F8SC	8D	89.3	98.2	13.9	15.2	11.2	0.64
		107		16.6		8.1	0.44
F8SX		124	106	19.2	16.4	7.5	0.83
		87.5		13.6		13.7	0.43
Mean of two tests; LES: loaded end slip; FES: free end slip; ld: embedded length							

III. Test Resuts and Discussions

The individual test results, obtained from the thirty two specimens tested in this study are tabulated in Tables 2 and 3 for ECC and FRC, respectively. All samples had the same GFRP bars, type of concrete for each group, and loading arrangement. The parameters investigated were: bar location, type of concrete, end case (straight or headed) and embedment length. Tables 2 and 3 summarize the test results in the form of the ultimate pullout force, bond stress and the corresponding load end-slip (LES) and free end-slip (FES) as well as the failure mode. The general mode of failure for all specimens was bar pullout through ECC and FRC or through the headed anchorage part.

A. Failure Modes, Pullout Loads, Load-slip Curves and Bond Strengths of ECC Group I

Table 2 summarizes the experimental results showing pullout/peak load, slip (at peak load) and bond stress of ECC specimens with GFRP bars embedded concentrically and eccentrically in the block. One specimen, with embedded length equal to 8D, was not used due to problems during testing.

Fig.5. *Slipping/pullout of GFRP bars for ECC specimens*

Fig. 6. *Slipping of GFRP bar from its headed end*

Fig. 5 and Fig. 6 show view of the GFRP bar slip at the bar-concrete block interface for both straight and headed bars, respectively. Fig. 7 and Fig. 8 show the load-slip relationships (free end slip 'FES' and loaded end slip 'LES') for both straight-end and headed-end bar (E8SX and $E4H_{ld}C$), respectively. From Fig. 6 and Fig.8, it is illustrated that the GFRP bar slipped from its head suddenly after the failure giving a large displacement.

For the straight bars with 4D, 6D and 8D embedment lengths, the average pullout loads were 20.75, 27.50 and 56 kN, respectively for concentric bars. However, they were about 23.63, 37.00 and 60.38 kN, respectively for eccentric bars. It can be observed that the pullout load increased by about 24.5% and 51% with the increase of embedment

length from 4D to 6D and 6D to 8D, respectively for concentric bars while this increase were 36% and 38.7%, respectively for eccentric bars.

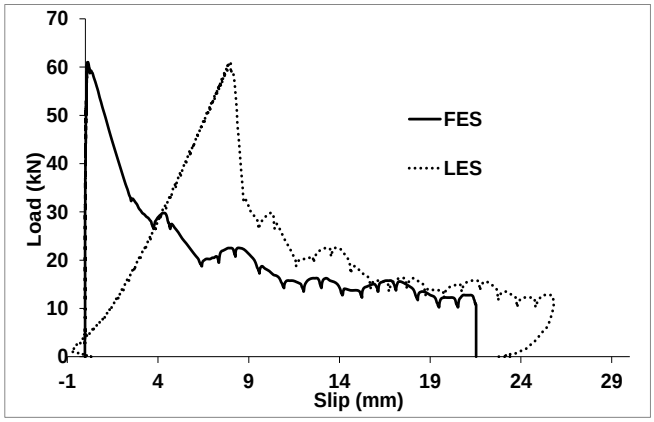

Fig.7. *Load-slip curve of E8SX*

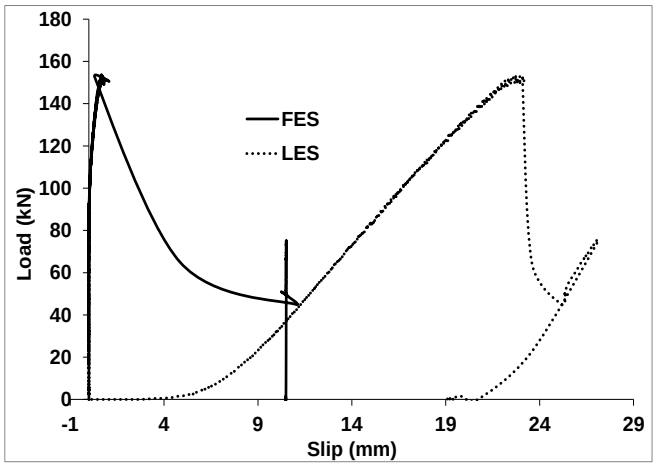

Fig. 8. *Load-slip curve of E4H$_{ld}$C*

The pullout loads for concentric bars were less than their eccentric counterparts by about 12%, 25% and 7% for 4D, 6D and 8D, respectively. The presence of the headed-end also enhanced the pullout load for both E4H$_0$C and E4H$_{ld}$C by 49% and 62%, respectively. Pullout load for headed end bar was also more than the failure load of E8SC with embedment length of 8D. This suggested that use of headed bars can significantly increase the pullout load.

Fig.9. *Slipping of GFRP bar for FRC specimens*

Fig.10. *Slipping of GFRP bar for headed end FRC specimens*

B. Failure Modes, Pullout Loads, Load-slip Curves and Bond Strengths of ECC Group II

Table 3 presents the experimental results showing pullout/peak load, slip at peak load and bond stress of FRC specimens with GFRP bars embedded concentrically and eccentrically in the block.

Fig. 9 and Fig.10 show GFRP bar slip at the bar-concrete block interface for both straight and headed bars, respectively.

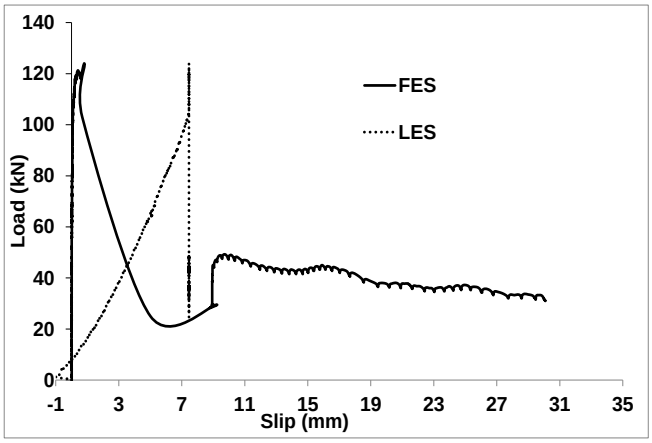

Fig.11. Load-slip curve of F8SX

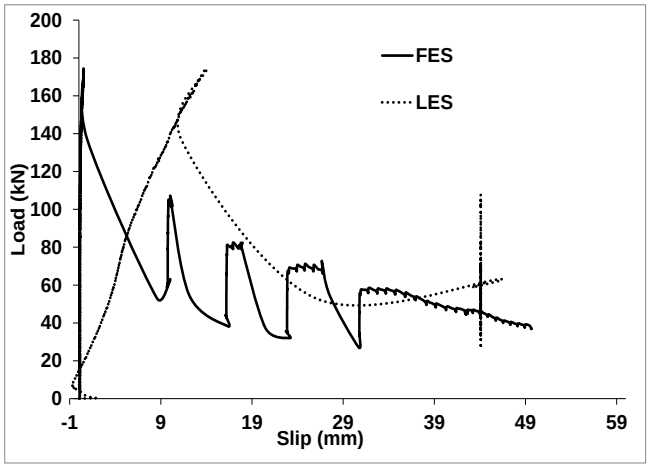

Fig.12. Load-slip curve of F4H$_{ld}$C

Fig.11 and Fig.12 show typical load-slip (FES and LES) relationships for both straight-end and headed-end bar (F8SX and E4H$_{ld}$C), respectively. It was

obvious from Fig.10 and Fig.12 that the GFRP bar slipped from its head suddenly after the failure producing a large displacement as was the case for ECC.

For the straight bars with 4D, 6D and 8D embedment lengths, the average pullout loads were about 52.75, 61.25 and 89.25 kN, respectively for concentric bars compared to about 58.63, 63.00 and 105.5 kN, respectively for eccentric bars. It can be observed that the pullout load increased by about 13.9% and 31.4% with the increase of embedment length from 4D to 6D and 6D to 8D, respectively for concentric bars while this increase were about 7% and 40%, respectively for eccentric bars.

The pullout loads for concentric bars were less than eccentric bars by about 10%, 3% and 15% for 4D, 6D and 8D, respectively. In addition, the presence of the headed-end enhanced the pullout load for both $F4H_0C$ and $F4H_{ld}C$ by 49% and 62%, respectively. In addition, the pullout load of headed end bar was more than the failure load for F8SC with embedment length equaled to 8D.

C. Comparison Between ECC and FRC Specimens based on Pullout Load

The average pullout load (P) was divided by the square root concrete compressive strength ($\sqrt{f_c}$) for all ECC and FRC specimens (about $\sqrt{55}$ and $\sqrt{75}$, respectively), to get the normalized load (P_n) as shown in Fig.13 and Fig.14 for straight and headed end bars, respectively.

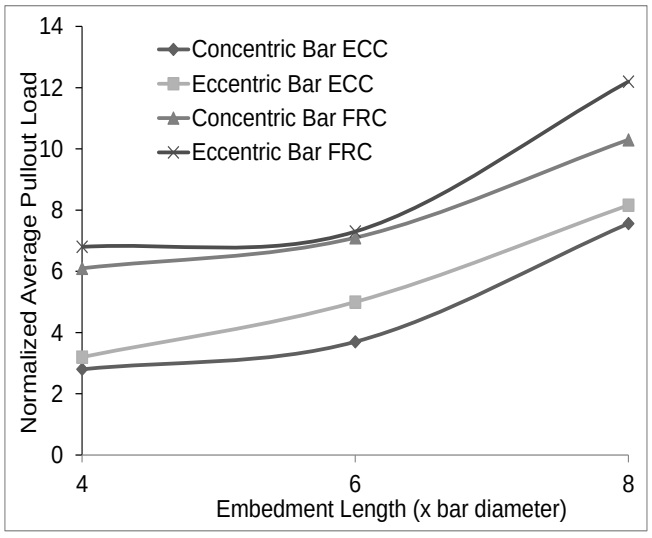

Fig. 13. Normalized pullout load for straight bars

Generally, the pullout load of the GFRP bars increased with the increase of embedment length (Fig. 13). Pullout loads of FRC specimens were higher than their ECC counterparts. This may be attributed to the higher concrete strength associated with the presence of large aggregates generating more interlocking and frictional forces in the bar-concrete interface. Another reason may be due to the pullout failure of the specimens rather the splitting failure. The higher pullout loads for eccentric bars compared to its concentric counterparts for both ECC and FRC specimens can be associated with the possible eccentric application of the pullout load causing simultaneous axial and bending load to the pullout specimens.

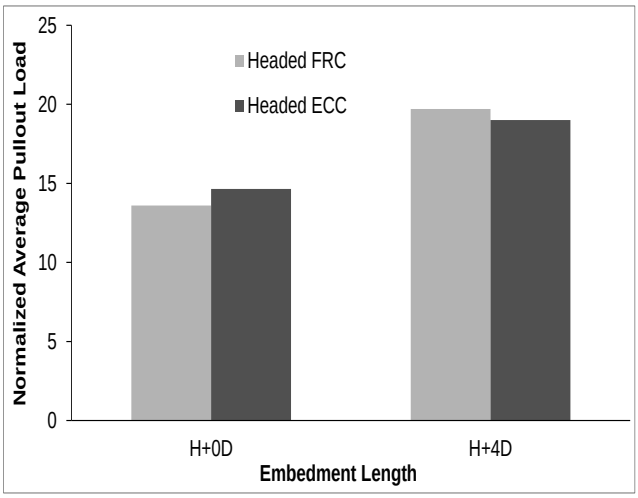

Fig. 14. *Normalized pullout load for headed-end bars*

Fig.14 compares the normalized pullout loads of headed-end bars with and without development length of 4D. The GFRP bar with headed-end + 4D showed significant increase in pullout strength compared to one with headed end without embedment length, as expected.

D. Comparison of Bond Stress Between ECC and FRC

Table 4 compares the bond stress of GFRP bars embedded in ECC and FRC. Bond strength slightly increased for ECC while decreased for FRC with the increase of development length from 4D to 8D.

Table 4. Comparison of Code predicted and experimental bond strength of ECC and FRC

	Bond strength (*T*) *MPa*				
Embed. Length 'ld'	**Expt.**	**CSA S806-02**		**ACI 440.1R-06**	
	T_{exp}	T_{CSA}	T_{exp}/T_{CSA}	T_{ACI}	T_{exp}/T_{ACI}
ECC specimens with concentric straight bar					
4D	*6.45*	*5.10*	*1.26*	*18.30*	*0.35*
6D	*5.70*		*1.12*	*13.14*	*0.43*
8D	*8.70*		*1.71*	*10.60*	*0.82*
ECC specimens with headed bar					
Headed	*21.87*	*5.10*	*4.29*	-	-
Headed + 4D	*17.91*		*3.51*	*18.30*	*0.98*
FRC specimens with concentric straight bar					
4D	*16.41*	*5.94*	*2.76*	*21.34*	*0.77*
6D	*12.70*		*2.13*	*15.36*	*0.83*
8D	*13.88*		*2.34*	*12.37*	*1.12*
FRC specimens with headed bar					
Headed	*23.39*	*5.94*	*3.93*	-	-
Headed + 4D	*20.68*		*3.48*	*21.34*	*0.97*

Bond stresses of GFRP bars embedded in ECC are found to be lower than those embedded in FRC. This can be attributed to combination of various factors such as higher

compressive strength of FRC, presence of coarse aggregate in FRC, higher confinement of FRC (due to presence of steel fiber and higher modulus of elasticity of FRC) and pullout nature of failure. Use of headed bar with and without development length increased the bond strength. But ECC specimens seemed to benefited more with 2.77 time increase in bond stress compared with 1.26 times increase in FRC specimens.

IV. Performance of Code Based Equations

The bond strength of ribbed GFRP bars embedded in ECC and FRC are calculated by using Canadian Code CSA S806-02 [18] and ACI 440.1R-06 [19] (based equations. Bond strength as per CSA S806-02 [18] is given by:

$$\tau_f = \frac{d_{cs}\sqrt{f_c'}}{1.15(K_1K_2K_3K_4K_5)\pi d_b} \quad (1)$$

where, τ_f is the FRP rebar-concrete effective bond strength; d_{cs} is the smallest of the distance from the closest concrete surface to the center of the bar being developed or two-thirds the centre to centre spacing of the bars being developed (mm) $d_{cs} \leq 2.5d_b$; f'c is the compressive strength of concrete (MPa); K_1 is bar location factor (1.3 for horizontal reinforcement placed so that more than 300 mm of fresh concrete is cast below the bar; 1.0 for all other cases); K_2 is concrete density factor (1.3 for structural low-density concrete; 1.2 for structural semi-low-density concrete; 1.0 for normal density concrete); K_3 is bar size factor (0.8 for < 300 Ab mm^2; 1.0 for > 300 A_b mm^2); K_4 is bar fiber factor (1.0 for GFRP); K_5 is bar surface profile factor (1.0 for surface roughened or sand coated or braided surfaces; 1.05 for spiral pattern surfaces or ribbed surfaces; 1.8 for indented surfaces); d_b is the bar diameter and A_b is the area of the bar.

Bond strength as per ACI 440.1R-06 [19] is as follows:

$$\frac{\tau}{\sqrt{f_c'}} = 0.33 + 0.025\frac{c}{d_b} + 8.3\frac{d_b}{l_{embed}} \quad (2)$$

where, τ is the FRP rebar-concrete effective bond strength; f'c is the compressive strength of concrete; c is the lesser of the cover to the center of the bar or one-half of the center-to-center spacing of the bars being developed; d_b is the bar diameter; and l_{embed} is the embedment length of the bar in concrete.

It should be noted that CSA S806-02 code does not take into consideration the effect of embedment length. However, the ACI Code permits this parameter for calculating bond strength oriented the bar. Since ACI (2) is developed based on concrete strength between 28 and 45 MPa, it cannot be assumed to be accurate for prediction of bond strength of ECC and FRC used in this study.

Table 4 compares bond stress predicted from Code (CSA S806-02) based equations and experiments. The Canadian code underestimates the bond strength of straight GFRP bars embedded in both ECC and FRC as experimental to predicted values ranges from 1.12 to 1.76 for ECC and from 2.13 to 2.76. The underestimation is even greater (for both ECC and FRC) for headed bars where the ratio of experimental to Code value is greater than 3.48. Canadian Code is therefore safe for the prediction of bond stress of GFRP bars in ECC and FRC. The ACI Code (ACI 440.1R-06) overestimates the bond strength of straight GFRP bars embedded in both ECC and FRC as experimental to predicted values ranges from 0.35 to 0.82 for ECC and from 0.77 to 1.12. ACI Code also overestimates the bond strength of headed GFRP bars and therefore, not safe.

V. Conclusions

This paper presents the bond behaviour of straight and headed ribbed GFRP bars embedded in engineered cementitious composite (ECC) and traditional fibre reinforced concrete (FRC). Experimental investigations were conducted using conventional pullout tests to evaluate the effects of embedment length and location of bar (concentric and eccentric) on the bond strength, pullout load and failure modes. The results from 96 pullout tests and Code based analyses lead to the following conclusions:

- All the specimens failed due to bar pullout. However, pullout in FRC specimen was sudden compared to gradual and significant ductile failure in ECC. The pullout load of GFRP bars increased with the increase of embedment length. FRC specimens showed higher pullout load compared to their ECC counterparts. GFRP bar with headed-end showed significant increase in pullout strength compared to the straight-end bar.
- Bond stresses of GFRP bars embedded in ECC are found to lower than those embedded in FRC. The use of headed end bar increased the bond strength. ECC specimens seemed to be benefited more with 2.8 time increase in bond stress compared to 1.26 times increase in FRC specimens.
- The Canadian code underestimates the bond strength of straight GFRP bars embedded in both ECC and FRC. The underestimation is even greater for headed bars where the ratio of experimental to Code value is greater than 3.48. Canadian Code is therefore safe for the prediction of bond stress of GFRP bars in ECC and FRC. On the other hand, the ACI Code overestimates the bond strength of both straight and headed GFRP bars in both ECC and FRC and therefore, not safe.
- The bond strength values of GFRP bars (with and without head) embedded in ECC and FRC can be used in the design of pre-fabricated bridges with GFRP reinforced closure strips. More investigations are necessary on this aspect and are currently in progress using full-scale bridge decks with ECC or FRC closure strips to fully understand the behavior.

ACKNOWLEDGMENT

Authors acknowledge the supports from Schoeck Canada Inc., King Packaged Materials Ltd. Canada and Egyptian Government. The supports received from lab technicians of Concrete and Structural Laboratories of Ryerson University Canada as well as research assistants are also acknowledged.

REFERENCES

[1] S. Gar, M. Head, S. Hurlebaus and J. Mander, Comparative experimental performance of bridge deck slabs with AFRP and steel precast panels", ASCE J. of Materials in Civil Engineering, Vol. 17, No. 6, 2013.

[2] V.C. Li, "Engineered cementitious composites (ECCs) – a review of the material and its application". Advanced Concrete Tech, Vol. 1, No. 3, p. 215–230, 2003.

[3] V.C. Li., S. Wang and C. Wu C., "Tensile strain-hardening behavior of PVA-ECC", ACI Material J., Vol. 98, No. 6, p.483–92, 2001

[4] J. Zhou, S. Qian, G. Ye, O. Copuroglu, K. Breugel, and V.C. Li, "Improved fiber distribution and mechanical properties of engineered cementitious composites by adjusting the mixing sequence", Cement & Concrete Composites, Vol.34, p.342-348, 2012.

[5] M. Sahmaran and V.C. Li, "Durability properties of micro-cracked ECC containing high volumes fly ash", Cement and Concrete Research, Vol. 39, p.1033–43, 2009.

[6] M. Şahmaran, M. Lachemi, K.M.A. Hossain and V.C. Li, "Influence of aggregate type and size on the ductility and mechanical properties of ECC, ACI Materials Journal, Vol. 106, No 3, p.308-316, 2009.

[7] M. Şahmaran, M. Lachemi, K.M.A. Hossain, R. Ranade and V.C. Li, "Internal curing of ECCs for prevention of early age autogenous shrinkage cracking, Cement and Concrete Research, Vol. 39, No. 10, P. 893-901, 2010.

[8] ACI Committee 408. Bond and development of straight reinforcing bars in tension. Farmington Hills, MI: American Concrete Institute, ACI 408R-03, 2003.

[9] M.H. Harajli, and K.A. Salloukh, "Effect of fibers on development/splice strength of reinforcing bars in tension", ACI Materials Journal, Vol. 94, No. 4, p. 317-324, 1997.

[10] A.N. Dancygier, A. Katz and U. Wexler, "Bond between deformed reinforcement and normal and high-strength concrete with and without fibers. Materials and Structures", Vol. 43, No.6, p. 839-856, 2010.

[11] W. Fuchs, R. Eligehausen and J. Breen, "Concrete capacity design (CCD) approach for fastening to concrete", ACI Structural Journal, Vol. 92, No. 1, p. 73-94, 1995.

[12] K.M.A. Hossain, D. Ametrano, C. Mak and M. Lachemi, "Bond strength and development length of GFRP bars in ultra-high performance concrete", Ministry of Transport Ontario (MTO) Technical Report (HIIFP Research Project), May, 89p, 2011.

[13] K.M.A. Hossain, C. Mak and D. Ametrano, "GFRP reinforced UHPC composites for sustainable bridge construction", Canadian Civil Engineer, Spring (29.1), p. 12-15, 2012.

[14] K.M.A. Hossain, D. Ametrano and M. Lachemi, "Bond strength of standard and high-modulus GFRP bars in high-strength concrete", ASCE J. of Materials in Civil Engineering, Vol. 26, No. 3, p.449-456, 2014.

[15] D-U Choi, S-U Chun, and S-S Ha, "Bond strength of glass fibre-reinforced polymer bars in unconfined concrete", Engineering Structures, Vol. 3, No. 1, p. 303-313, 2012.

[16] Shoeck Canada Inc., http:// www.schoeck.ca (Access date: 14-08-2014)

[17] RILEM. "RC 6 bond test for reinforcement steel. 2. Pull-out test, 1983. Recommendations for the testing, and use of constructions materials, E & FN Spon, London, 1994.

[18] CSA S806-12, "Design and construction of building components with fibre reinforced polymers, Rexdale, ON, Canadian Standards Association, Rexdale, Canada, 2012.

[19] ACI Committee 440 (2006). Guide for the design and construction of structural concrete reinforced with FRP bars (ACI 440.1R-06). Farmington Hills, MI: American Concrete Institute.